Electronic Supplementary Material (ESI) for RSC Advances.
This journal is © The Royal Society of Chemistry 2022

Supporting Information

A novel metal-organic framework of Ba-hemin with enhanced cascade activity for sensitive glucose detection

Jintao Yi*[a], Xianqin Han[a], Fengying Gao[a], Le Cai[a], Ying Chen[a], Xiulong Deng[a], Xun Li*[a], Jun Xue*[a] and Hui Zhou*[ab]

[a.]Key Laboratory of Organo-Pharmaceutical Chemistry of Jiangxi Province, Gannan Normal University, Ganzhou 341000, P. R. China

[b.]Guangdong Provincial Key Laboratory of Research and Development of Natural Drugs, and School of Pharmacy, Guangdong Medical University, Dongguan 523808, PR China

E-mail: yistarthappy@163.com; Fax: (+86)797-8393536; Tel: +86-797-8393536

Table S1 A comparison of the analytical performance of Ba-hemin@GOX using other colorimetric sensors for glucose detection.

Materials	Linear range for glucose (M)	Detection limit for glucose (μM)	Reference
Fe_3O_4 particles	$5 \times 10^{-5} – 1 \times 10^{-3}$	30	26
Cellulose-strips	$1 \times 10^{-3} – 1.1 \times 10^{-2}$	450	27
Graphene aerogel	$1 \times 10^{-3} – 1.8 \times 10^{-2}$	870	28
Silicon-GOX	$1 \times 10^{-3} – 1.5 \times 10^{-2}$	330	29
MOF-808	$5.7 \times 10^{-6}–1.7 \times 10^{-3}$	5.7	30
Ba-hemin@GOX	$9.3 \times 10^{-6}–7.4 \times 10^{-4}$	3.1	This work

Table S2 Results of the detection of glucose in tap water, serum and drink.

Sample	Added (mM)	Founded (mM)	Recovery (%)	RSD (%, n=3)
Tap water	0.037	0.041	110.8	3.6
	0.074	0.075	101.4	4.2
	0.185	0.189	102.2	2.9
	0.370	0.387	104.6	5.3
	0.555	0.572	103.1	1.6
	0.740	0.681	92.0	4.8
Serum	0.037	0.035	94.6	1.5
	0.074	0.077	104.1	3.1
	0.185	0.192	103.8	4.6
	0.370	0.397	107.3	5.4
	0.555	0.547	98.6	3.6
	0.740	0.739	99.9	2.8
Drink	0.037	0.037	100.0	3.2
	0.074	0.075	101.4	4.5
	0.185	0.192	103.8	1.9
	0.370	0.357	96.5	5.3
	0.555	0.556	100.2	2.6
	0.740	0.755	102.0	3.8

Fig.S1 The synthesis optimization of Ba-hemin with different molar ratios, (A) The illustration of the synthesis of Ba-hemin, (B) The SEM images.

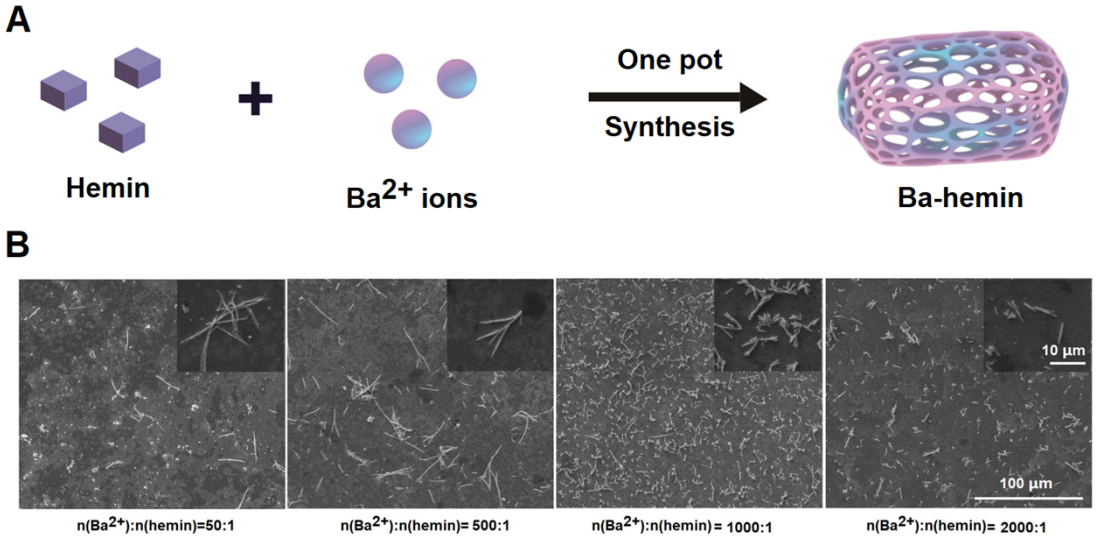

Fig.S2 The UV-vis absorbance spectrum of Ba-hemin.

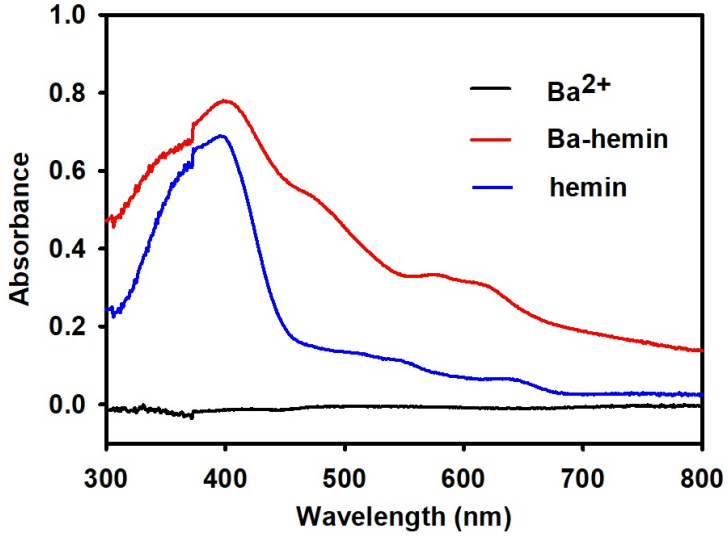

Fig.S3 The peroxidase-like catalytic activity detection of Ba-hemin with the different concentrations of H_2O_2. (A) The UV-vis absorbance spectrum, (B) The corresponding double reciprocal plot.

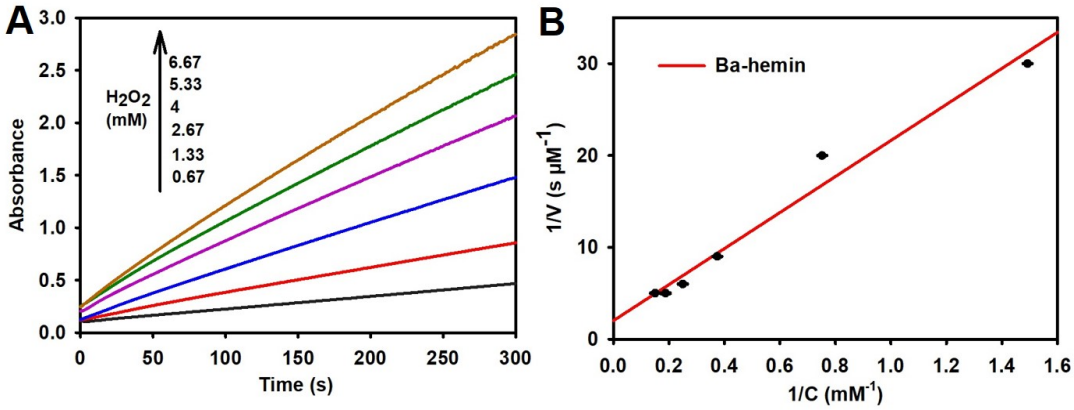

Fig.S4 The peroxidase activity detection of horseradish peroxidase (HRP) with the different concentrations of H_2O_2. (A) The UV-vis absorbance spectrum, (B) The corresponding double reciprocal plot.

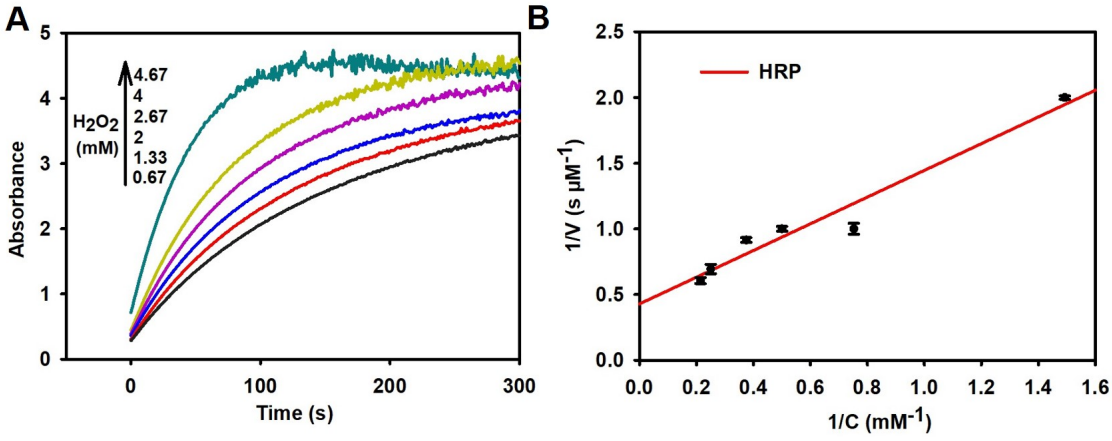

Fig.S5 The TGA of Ba-hemin and Ba-hemin@GOX.

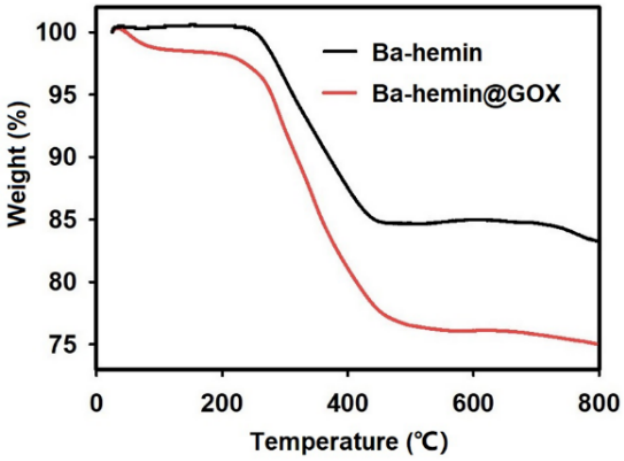

Fig.S6 The FTIR spectras of GOX, Ba-hemin@GOX, Ba-hemin/GOX, Ba-hemin/GOX+SDS, Ba-hemin.

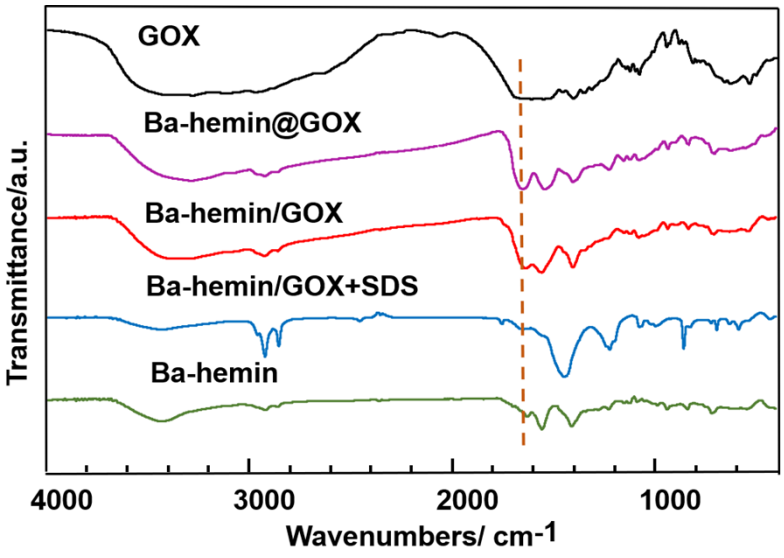

Fig.S7 The fluorescence intensity detections of the Ba-hemin@FITC-GOX and the unreacted FITC-GOX.

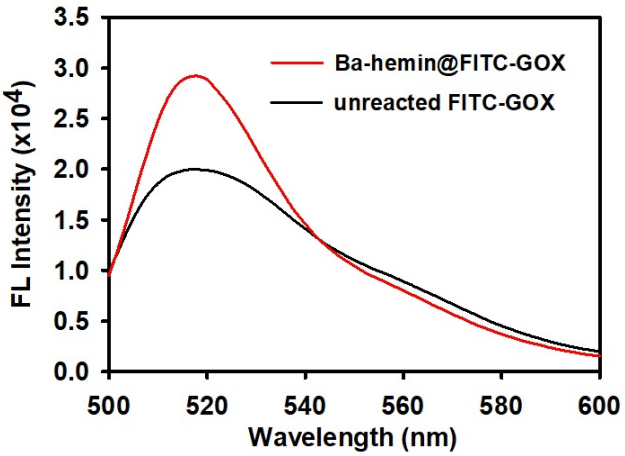

Fig.S8 The double reciprocal plots of the activity of (A) free GOX and (B) Ba-hemin@GOX with the concentration of glucose.

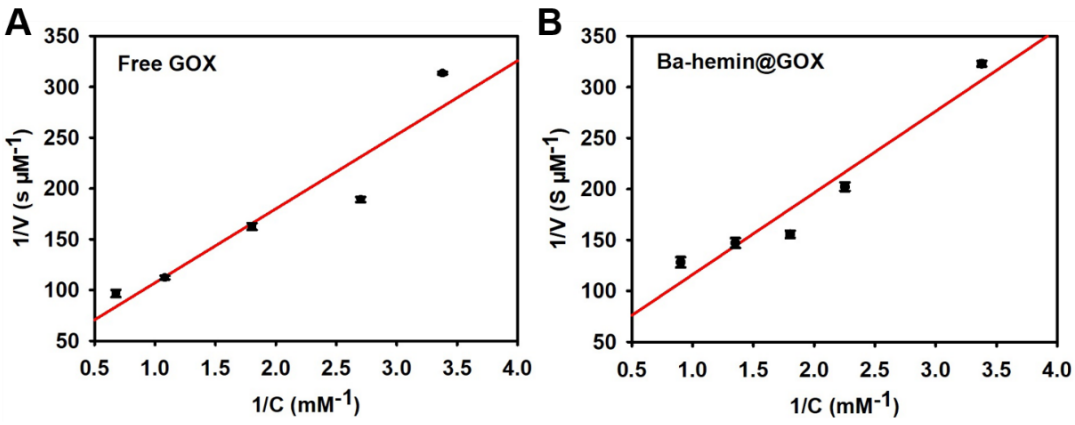

Fig.S9 The effect of (A) temperature and (B) pH on the activity of Ba-hemin@GOX (red line) and free GOX (black line). The error bars represent the standard deviation of three measurements.

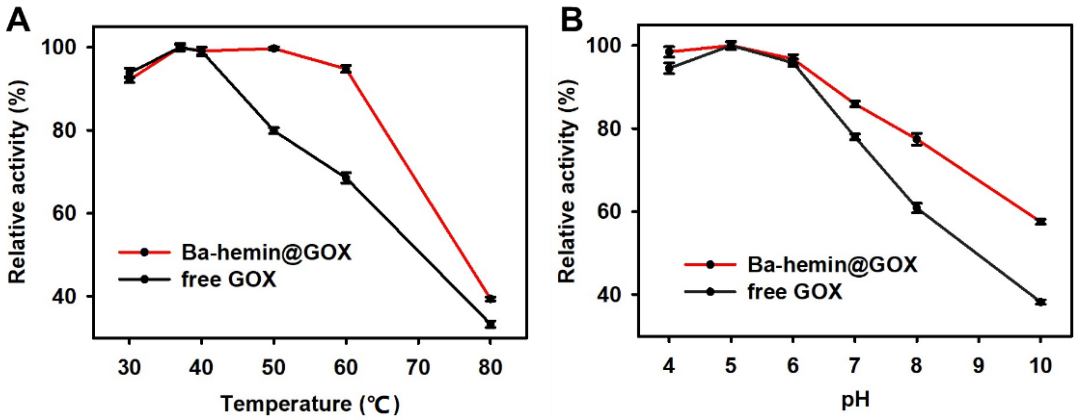

Fig.S10 The storage stability of Ba-hemin@GOX with different days.